

Parity nonconserving two-pion exchange in elastic proton-proton scattering

J. A. Niskanen,^{1,*} T. M. Partanen,^{1,†} and M. J. Iqbal²

¹ *Department of Physical Sciences, P. O. Box 64,
FIN-00014 University of Helsinki, Finland*

² *Department of Physics and Astronomy,
University of British Columbia, Vancouver, BC, Canada, V6T 1Z1*

(Dated: February 2, 2008)

Abstract

Parity nonconserving two-pion exchange in elastic $\vec{p}p$ scattering is investigated in the presence of phenomenological strong distortions in various models. Parity violation is included in $NN\pi$ vertex considering NN and $N\Delta(1232)$ intermediate states in box and crossed box diagrams. Using the derived parity nonconserving two-pion exchange potential we calculate the longitudinal analyzing power \bar{A}_L in elastic pp scattering. The predicted effect is of the same order as vector meson exchanges.

PACS numbers: 11.30.Er, 13.75.Cs, 21.30.Cb, 13.75.Gx, 24.70.+s, 25.40.Cm

*Electronic address: jouni.niskanen@helsinki.fi

†Electronic address: tero.partanen@helsinki.fi

I. INTRODUCTION

Although the basic weak interaction is relatively well known, there exist large uncertainties of the weak couplings of mesons and baryons at the hadron level relevant at low and intermediate energies up to about 1 GeV, *i.e.* in nuclear physics. For example the efforts to determine the parity nonconserving (PNC) couplings [1, 2] report uncertainties of the order of 100 % or more of the recommended "best" values. (For reviews see *e.g.* Refs. [3, 4].) In this situation even the signs of couplings may be suspect.

Considering the weakness of the couplings their experimental determination is a big challenge and attempts often utilize nuclear structure to enhance PNC effects. However, the analysis of the basic couplings is then complicated by the environment. Among few-nucleon systems also polarized photoreactions have been used with the deuteron.

In principle, the most direct way without external disturbances would be NN scattering. Presently PNC np scattering experiments are unlikely and even pp scattering experiments are scarce [5, 6, 7, 8]. Among these of particular interest is the measurement of the parity violating spin observable \bar{A}_L in the TRIUMF experiment E497 at 221.3 MeV [8]. The energy was chosen so that incidentally the strong interaction phases conspire to cause the $J = 0$ contribution to cross zero [9]. While in this amplitude both ρ and ω mesons are equally important, the next $J = 2$ parity mixing amplitude is strongly dominated by ρ exchange enabling a drive towards PNC ρpp coupling.

The above logic is based on the idea that the dominant PNC effect in pp scattering should be due to vector mesons, since long-ranged single pion exchange is forbidden by Barton's theorem [10]. This theorem forbids in general neutral 0^\pm mesons to couple with nucleons in the PNC interaction because of the simultaneous violation of \mathcal{P} and \mathcal{CP} symmetries. So in the PNC pp interaction at low energies only ρ -, and ω -meson exchanges are expected to be significant and the two-pion exchange (TPE) is assumed negligible [3]. With these assumptions the TRIUMF experiment E497 [8] would, in principle, result in the determination of the weak ρpp coupling constant $h_\rho^{pp} = h_\rho^{(0)} + h_\rho^{(1)} + h_\rho^{(2)}/\sqrt{6}$ from pp scattering. The lower energy experiments [5, 6] have already determined the independent combination of $h_\rho^{pp} + h_\omega^{pp}$ (where $h_\omega^{pp} = h_\omega^{(0)} + h_\omega^{(1)}$) and so both the h_ρ^{pp} and h_ω^{pp} are supposedly determined separately.

In view of such dedicated and very time consuming experiments it is important to carefully study the validity of the assumptions and uncertainties in their interpretation. In fact, it was shown in Ref. [11] that Δ -isobar excitation by weak ρ and strong (mainly) pion exchange has a significant effect on \bar{A}_L at all energies and should also be considered. In spite of PNC single pion exchange being excluded in pp scattering, crossed charged two-pion exchange is allowed. Charged pions are also possible in two-pion exchanges involving the excitation of the $\Delta^{++}(1232)$ resonance. The former was studied already in the early works [12, 13], while calculations for the latter were performed above the pion production threshold in Refs. [14, 15]. However, the Δ contribution extends also below this to low energies (as shown with vector meson exchanges in Ref. [11]). To our knowledge the contribution of all these two pion effects to PNC observables has not been investigated systematically on the same footing together. Closest comes the recent Ref. [16] in deriving PNC the two-pion potential in chiral perturbation theory. Our aim in the present paper is to calculate this potential including realistic form factors and extending the calculation to the observable \bar{A}_L . Further interest in TPE lies in the fact that it should be the longest ranged PNC effect in pp scattering, which might show up in energy dependence.

The organization of the paper is as follows. First we evaluate numerically PNC TPE

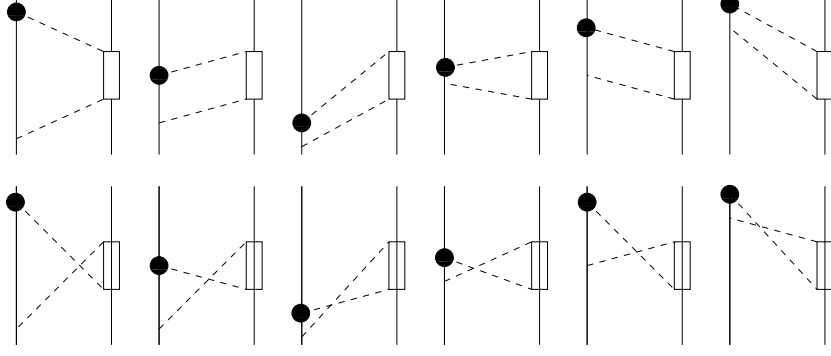


FIG. 1: Time orderings of parity nonconserving (black spot) two-pion exchange (dashed line) via nucleon (solid line) delta ($\bar{\Delta}$) intermediate state. Both the crossed and box graphs include the $N\Delta$ intermediate state while the NN intermediate state can appear only in the crossed graphs. The direction of time is upwards.

as a potential in the momentum representation assuming the baryons to be static. This potential can be well fitted by Lorentz functions of the momentum transfer, which in turn can be expressed in terms of Yukawa functions in the coordinate representation. It may be noted that the result will be local (excluding relativistic corrections) and a comparison with the local parts of vector meson exchanges is then straightforward. Next we discuss non-static effects in three different kinematics and dynamics allowing kinetic energies for baryons. These are found to be significant but not necessarily dominant.

II. THEORY

A. Basic interactions

The Hamiltonians for the parity conserving (PC) πNN , $\pi N\Delta$, and PNC πNN interactions, which describe the needed nonrelativistic vertices are

$$\mathcal{H}_{NN\pi}^{\text{PC}} = \frac{if_\pi}{m_\pi} N^\dagger \boldsymbol{\sigma} \cdot \mathbf{q} \boldsymbol{\tau} \cdot \boldsymbol{\pi} N, \quad (1)$$

$$\mathcal{H}_{N\Delta\pi}^{\text{PC}} = \frac{if_\pi^*}{m_\pi} \Delta^\dagger \mathbf{S} \cdot \mathbf{q} \mathbf{T} \cdot \boldsymbol{\pi} N + \text{h.c.}, \quad (2)$$

$$\mathcal{H}_{NN\pi}^{\text{PNC}} = \frac{h_\pi^{(1)}}{\sqrt{2}} N^\dagger (\boldsymbol{\tau} \times \boldsymbol{\pi})_0 N. \quad (3)$$

In this calculation only the NN and $N\Delta$ intermediate states are considered and $\Delta\Delta$ intermediate state ignored, because the PNC $N\Delta\pi$ vertex is concluded to be very small in Ref. [17]. We take it to be zero.

Unfortunately, in literature choices of the signs in the above definitions vary, both overall and even in the πNN *vs.* $\pi N\Delta$ vertices. In purely strong interactions the signs cancel, but in the presence of a weak vertex the sign matters. Our choice follows the standard one (DDH [1]) so that our PNC OPE potential

$$V_{NN\pi}^{\text{PNC}}(\mathbf{r}) = \frac{h_\pi^{(1)} f_\pi}{\sqrt{2} m_\pi} (\boldsymbol{\tau}_1 \times \boldsymbol{\tau}_2)_0 (\boldsymbol{\sigma}_1 + \boldsymbol{\sigma}_2) \cdot \hat{\mathbf{r}} \frac{\partial}{\partial r} Y_\pi(r) \quad (4)$$

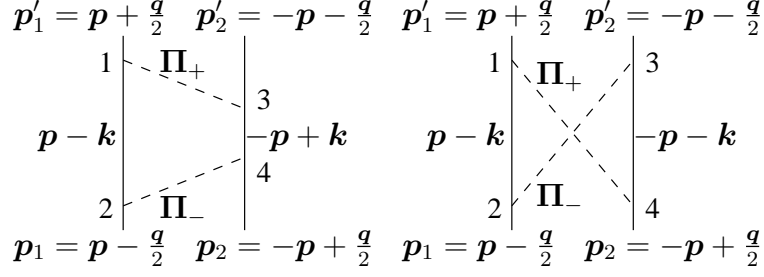


FIG. 2: The symmetry of the kinematics for the box and crossed graphs, where \mathbf{q} is the momentum transfer, \mathbf{k} the free loop momentum, and \mathbf{p} the relative momentum between the nucleons. The pions carry the momentum $\mathbf{\Pi}_{\pm} = \mathbf{k} \pm \frac{\mathbf{q}}{2}$. Numbers 1-4 denote respectively the number of the vertex.

would be as given in *e.g.* Ref. [3]. Here $Y_{\pi}(\mathbf{r})$ represents the Yukawa function $Y_{\pi}(\mathbf{r}) = e^{-m_{\pi}r}/4\pi r$ (possibly modified by a form factor).

The change of the πNN coupling to the $\pi\Delta N$ would be a replacement of the nucleon spin-isospin operators $\boldsymbol{\sigma}$ and $\boldsymbol{\tau}$ by the transition operators \mathbf{S} and \mathbf{T} with the normalization $S_i^{\dagger}S_j = (2\delta_{ij} - i\epsilon_{ijk}\sigma_k)/3$ [18].

Time orderings of the PNC TPE via $N\Delta$ intermediate state can be grouped under eight different groups, which all contain six time orderings that have the same spin and isospin structure. Two of the groups correspond to the graphs in Fig. 1, where the upper row is for the box (B) and the lower for the crossed (C) graphs, in which the parity is broken in vertex 1 (the vertices are numbered in Fig. 2). The rest of the groups can also be formed by using the graphs in Fig. 1: Two of the groups include the same graphs except the parity is broken in vertex 2. The remaining four groups can be obtained in the same manner from Fig. 1 with the exchange $N \leftrightarrow \Delta$ and breaking the parity respectively in vertices 3 and 4. Time orderings of the PNC TPE via NN intermediate state correspond only to the crossed graphs in Fig. 1. This contribution has four different groups, *i.e.* the parity is broken once in each vertex. Overall there are totally 72 time-ordered graphs to add up.

A symmetric and practical choice of the meson mediated momentum transfers is $\mathbf{\Pi}_{\pm} = \mathbf{k} \pm \frac{\mathbf{q}}{2}$ shown in Fig. 2, where \mathbf{k} is an integration parameter and \mathbf{q} the overall momentum transfer.

B. Static model

In our basic model the initial and final nucleons and all the intermediate baryons are considered static. The energy (mass) difference between the isobar and nucleon is denoted by $\delta = M_{\Delta} - M$ and the energies of the exchanged pions are $w_{\pm} = (m_{\pi}^2 + \mathbf{\Pi}_{\pm}^2)^{\frac{1}{2}}$. The energy denominators of the different graph types given in Fig. 1 act as propagators of the 'old-fashioned' time ordered second-order perturbation theory

$$\mathcal{D}_{N\Delta}^B(\mathbf{k}, \mathbf{q}) = -\frac{1}{4w_+w_-} \left\{ \frac{1}{\delta} \left[\frac{1}{w_+ + \delta} + \frac{1}{w_+} \right] \left[\frac{1}{w_- + \delta} + \frac{1}{w_-} \right] + \frac{1}{w_+ + w_-} \left[\frac{1}{w_+(w_- + \delta)} + \frac{1}{w_-(w_+ + \delta)} \right] \right\},$$

$$\begin{aligned}
\mathcal{D}_{N\Delta}^C(\mathbf{k}, \mathbf{q}) &= -\frac{1}{4w_+w_-} \left\{ \frac{1}{w_+ + w_-} \left[\frac{1}{w_+(w_+ + \delta)} + \frac{1}{w_-(w_- + \delta)} \right] \right. \\
&\quad \left. + \frac{1}{\delta + w_+ + w_-} \left[\frac{1}{w_+ + \delta} + \frac{1}{w_-} \right] \left[\frac{1}{w_- + \delta} + \frac{1}{w_+} \right] \right\}, \\
\mathcal{D}_{NN}^C(\mathbf{k}, \mathbf{q}) &= -\frac{1}{2w_+w_-} \left\{ \frac{1}{w_+w_-} + \frac{1}{w_+^2} + \frac{1}{w_-^2} \right\} \frac{1}{w_+ + w_-}.
\end{aligned} \tag{5}$$

Each of these propagators corresponds also to a different spin-isospin structure acting in the numerator. However, a simplification arises from the even parity of the propagators, which does not affect PNC. Then their angular dependence is only due to $\cos^2 \theta_{kq}$, which in a good approximation can be taken the angular average $1/3$ (*i.e.* one can replace $\cos \theta_{kq} \rightarrow \sqrt{1/3}$). Thus PNC actually arises from the vertex structure of Eqs. (1)–(3). In fact, only the terms with even powers of k survive, when the angular integral is carried out.

In momentum space the resulting PNC TPE potential is obtained in the local form

$$\tilde{V}_{NN2\pi}^{\text{PNC}}(\mathbf{q}) = ih_\pi^{(1)} (\boldsymbol{\sigma}_1 \times \boldsymbol{\sigma}_2) \cdot \mathbf{q} \tilde{U}(\mathbf{q}) \tag{6}$$

with

$$\tilde{U}(\mathbf{q}) = -\frac{4f_\pi^3(\boldsymbol{\tau}_1 + \boldsymbol{\tau}_2)_0}{75\sqrt{2}\pi^2 m_\pi^3} \int_0^\infty dk \mathbf{k}^4 (12\mathcal{D}_{N\Delta}^B - 4\mathcal{D}_{N\Delta}^C + 25\mathcal{D}_{NN}^C). \tag{7}$$

Here we have used the quark model relation $f_\pi^* = \sqrt{\frac{72}{25}} f_\pi$ between the strong transition coupling and the πNN coupling [18]. The isospin operator contributes a factor of +2 in the case of elastic proton-proton scattering.

We calculate Eq. (7) executing the integral numerically with a monopole form factor of the type

$$F_\pm(\mathbf{k}, \mathbf{q}) = \frac{\Lambda_\pi^2 - m_\pi^2}{\Lambda_\pi^2 + \mathbf{\Pi}_\pm^2} \tag{8}$$

included in each vertex. The parameters given in Table I are used to calculate $\tilde{U}(\mathbf{q})$ with $f_\pi = m_\pi g_\pi / 2M$, the charged pion mass $m_\pi = 139.6$ MeV and the average nucleon mass $M = 939$ MeV. The relatively small cut-off mass of the pion is in line (even harder) with the cloudy bag size arguments [20, 21, 22, 23] and its use here does not conflict with the Bonn potential parameters used for the vector mesons.

TABLE I: Parameter values for meson-nucleon couplings. The weak couplings h_α^{pp} , $\alpha = \pi, \rho, \omega$ ($h_\pi^{(1)}$ for pions), are the "best" estimates of Refs. [1] (DDH) and [2] (FCDH). The strong couplings and cut-offs of the vector mesons are from the coordinate space OBE of Ref. [19].

	DDH	FCDH			
	$h_\alpha^{pp} (10^{-7})$	$h_\alpha^{pp} (10^{-7})$	$g_\alpha^2/4\pi$	χ_α	Λ_α (GeV)
π	4.6	2.7	13.8	-	1.0
ρ	-15.5	-7.0	0.95	6.1	1.3
ω	-3.0	-7.2	20	0	1.5

TABLE II: Fit parameters for the Eq. (11) for the static partial contributions and the non-static total contributions in two different kinematics.

	A (fm ³)	B (fm ⁻¹)	C (fm ⁻¹)
STATIC			
$N\Delta^B$	0.148934	3.5987	10.8463
$N\Delta^C$	-0.0170383	3.18247	8.28774
NN^C	0.226128	2.77668	7.59613
NON-STATIC			
symmetric	0.215807	2.74463	23.6659
asymmetric	0.215388	2.13806	6.32248

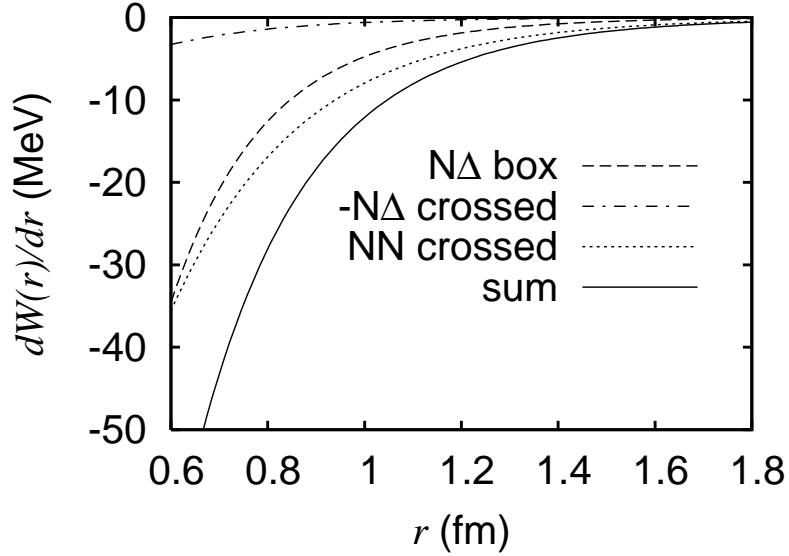


FIG. 3: The total and the partial contributions of the PNC TPE given by Eq. (11).

We fit separately all the three pieces of Eq. (7), which represent contributions of the different graph types, to see their relative strengths. Excellent fits (relative error $\leq 1\%$) are achieved with the function of the form

$$\tilde{W}(\mathbf{q}) = A \frac{B^2}{B^2 + \mathbf{q}^2} \left(\frac{C^2}{C^2 + \mathbf{q}^2} \right)^2. \quad (9)$$

with the parameter values given in Table II.

Following Ref. [24] we replace Eq. (7) with the fit in (6) and get the configuration space potential as the Fourier transform

$$V_{pp2\pi}^{\text{PNC}}(\mathbf{r}) = h_{\pi}^{(1)}(\boldsymbol{\sigma}_1 \times \boldsymbol{\sigma}_2) \cdot \hat{\mathbf{r}} \frac{\partial}{\partial r} W(\mathbf{r}) \quad (10)$$

with

$$\frac{\partial}{\partial r} W(\mathbf{r}) = \frac{AB^2}{4\pi} \left(\frac{C^2}{C^2 - B^2} \right)^2 \left\{ e^{-Cr} \left[\frac{C^2 - B^2}{2} + \frac{1}{r} \left(C + \frac{1}{r} \right) \right] - \frac{e^{-Br}}{r} \left(B + \frac{1}{r} \right) \right\}. \quad (11)$$

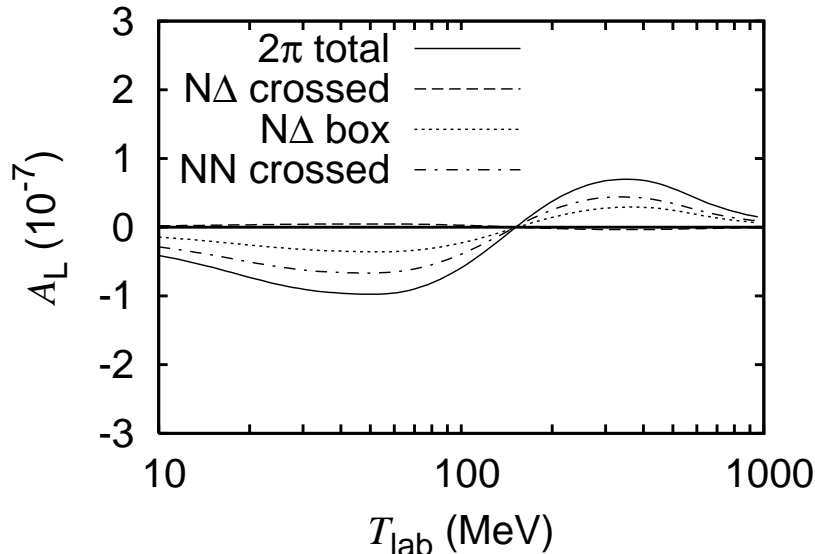


FIG. 4: The analyzing power \bar{A}_L arising from the different partial contributions of the PNC 2π exchanges using the DDH "best" value for the weak coupling $h_\pi^{(1)}$.

The magnitudes of Eq. (11) for the partial contributions are illustrated in Fig. 3, where the NN crossed box and ΔN direct box are by far dominant. As expected, the crossed NN contribution is of the longest range, but the ΔN excitation becomes as important or even larger inside 0.6 fm. Partly due to the weight factors present in Eq. (7) the crossed ΔN contribution is nearly negligible.

A comparison with the potential obtained from chiral perturbation theory [16] may be in order. That contains also the (reducible) box diagram and a triangle diagram with s -wave rescattering. The former is identically zero in pp scattering (Barton's theorem), while the latter is chirally suppressed in the pp case. So our results should be similar. In fact, for distances larger than about 1.2 fm they are indistinguishable, whereas inside the radius of 0.8 fm our result is significantly softer due to the form factors involved. Both have a range corresponding roughly to vector meson exchanges, so actually probably one may expect similar results.

We now use the above PNC 2π exchange potential to calculate the asymmetry of the parity-violating spin observable

$$\bar{A}_L = \frac{\sigma^+ - \sigma^-}{\sigma^+ + \sigma^-}, \quad (12)$$

where σ^\pm are the scattering cross sections of the two helicity states of the longitudinally polarized beam. The Reid soft-core potential [25] is used to obtain the strong interaction distortions for weak interactions, while to minimize theoretical uncertainties otherwise the empirical phase shifts and strong interaction amplitudes are used and taken from Ref. [26]. It has been seen in the past that the dependence on the strong potential is relatively weak and we do not go in this in detail [27, 28]. Therefore, apart from the easily scalable πNN weak coupling and the form factor, the results in Fig. 4 may be considered fairly model independent. Contributions of the five lowest parity mixed partial wave amplitudes ($^1S_0 - ^3P_0$), ($^3P_2 - ^1D_2$), ($^1D_2 - ^3F_2$), ($^1G_4 - ^3F_4$), and ($^1G_4 - ^3H_4$) are included in this calculation. Structurally the $J = 0$ and $J = 2$ contributions are similar to earlier results and the

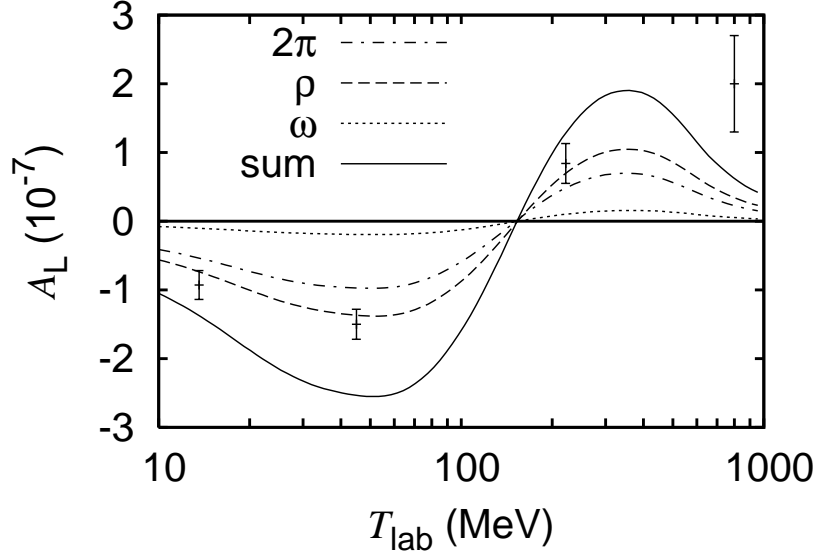


FIG. 5: Analyzing power \bar{A}_L for the PNC TPE and the local parts of the ω and ρ exchanges using the DDH "best" values for the weak couplings. The experimental data points are Bonn at 13.6 MeV [29], PSI at 45 MeV [5], TRIUMF at 221.3 MeV [8], and Los Alamos at 800 MeV [7].

expansion is already converged for those ($J = 4$ is negligible at our energies).

As the TPE effect in \bar{A}_L is clearly large, it is of utmost interest to compare the present result against vector meson effects considered earlier. These potentials are given in Ref. [1] in which we also incorporate the monopole form factors of the type (8) in each vertex and use two sets of weak couplings [1, 2]. Thus the PNC vector meson potentials for ρ and ω read

$$V_{pp\alpha}^{\text{PNC}}(\mathbf{r}) = -\frac{g_\alpha h_\alpha^{pp}}{M} \left((\boldsymbol{\sigma}_1 - \boldsymbol{\sigma}_2) \cdot \{-i\boldsymbol{\nabla}, Y_\alpha(\mathbf{r})\} + i(1 + \chi_\alpha)(\boldsymbol{\sigma}_1 \times \boldsymbol{\sigma}_2) \cdot [-i\boldsymbol{\nabla}, Y_\alpha(\mathbf{r})] \right), \quad (13)$$

$$Y_\alpha(\mathbf{r}) = \frac{e^{-m_\alpha r}}{4\pi r} - \frac{e^{-\Lambda_\alpha r}}{4\pi} \left(\frac{1}{r} + \frac{\Lambda_\alpha^2 - m_\alpha^2}{2\Lambda_\alpha} \right) \quad (14)$$

with the relevant parameters given in Table I. In the case of the vector mesons we use only the dominant local (latter) term of Eq. (13) and neglect its nonlocal (former) term, which only causes a minor contribution on the interaction [27] and also does not have a direct correspondence with the present local interaction. The PNC TPE effect is comparable in size to those given by vector meson exchanges using both sets (Figs. 5 and 6). The older set (DDH) would give the sum as an overestimate, while the new analysis (FCDH) gives a satisfactory agreement. However, one should remember that the nonlocal PNC would increase the result somewhat.

C. Non-static effects

So far the calculation has totally neglected any kinetic energies of baryons. This assumption gives simplicity and clarity while still being probably reasonably realistic due to the large baryon masses. We now make various attempts to overcome this approximation and to model non-static effects.

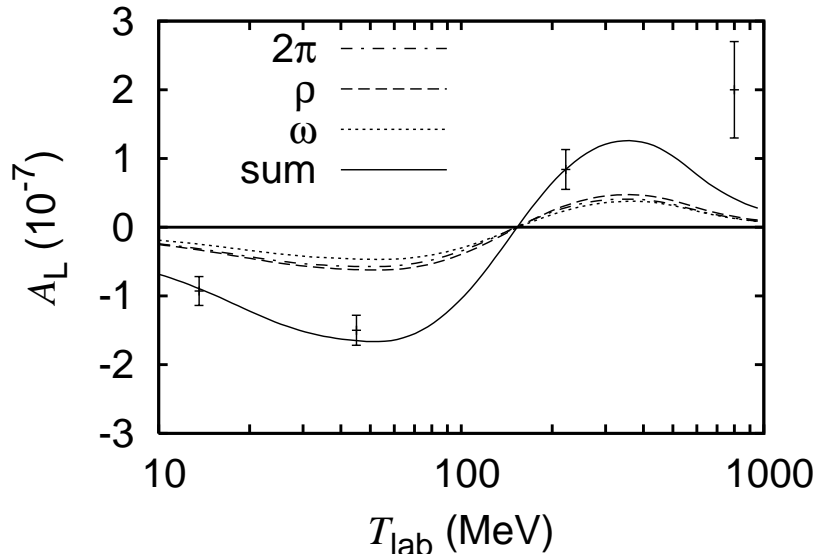


FIG. 6: The same as Fig. 5, except the FCDH 'best' values are employed. The 2π and ρ exchanges are now nearly indistinguishable.

First we still take the initial kinetic energy (and baryon momenta) to be zero, while the intermediate and final baryons have nonzero energies. In this case the final relative momentum is \mathbf{q} and energy is not conserved. In one boson exchange potentials without internal excitations this is not a problem and presently we are just making an energy independent potential. The relatively trivial generalization of Eq. (5) with $\mathbf{p} = \mathbf{q}/2$ in Fig. 2 yields a qualitatively similar but weaker potential, since the excitation is larger, and a smaller \bar{A}_L ("non-static asymmetric" dashed curve in Fig. 7 and parametrization in Table II).

Another way of considering non-static effects is to allow kinetic energy to be present in the initial state with the consequences on momenta. In this case the assumption of the conservation of energy would give a simplification making \mathbf{p} and \mathbf{q} orthogonal and kinematics could be symmetric. However, in this case numerically one meets a pole in the integration over \mathbf{k} at higher energies, *i.e.* for large incident momenta. Taking for definiteness \mathbf{p} to be zero it is, nevertheless, possible to get a result without the pole disturbing too much numerics (keeping $q \leq 5 \text{ fm}^{-1}$) – see Fig. 7 (dotted curve) and Table II.

Probably the best way to include the kinetic energy of the baryons is to incorporate them dynamically in the equation of motion. This can be done at the two-baryon level by the coupled-channel Schrödinger equation. Although this does not cover crossed mesons, following Ref. [24] it is possible to rearrange the direct and crossed ΔN diagrams as

$$\mathcal{N}_B \mathcal{D}_B + \mathcal{N}_C \mathcal{D}_C = \mathcal{N}_B (\mathcal{D}_B + \mathcal{D}_C) + (\mathcal{N}_C - \mathcal{N}_B) \mathcal{D}_C, \quad (15)$$

where the numerators involving the spin-isospin structure are denoted by \mathcal{N} . The first term is an iteration of static π exchange potentials, since the sum of all propagators turns out to be just $-(\omega_+^2 \delta \omega_-^2)^{-1}$ and \mathcal{N}_B has the corresponding vertex structure. So this term can be generated by coupled channels iterating an $NN \leftrightarrow \Delta N$ transition potential, while the second is presumably a smaller residual correction to be dealt with perturbatively. In terms

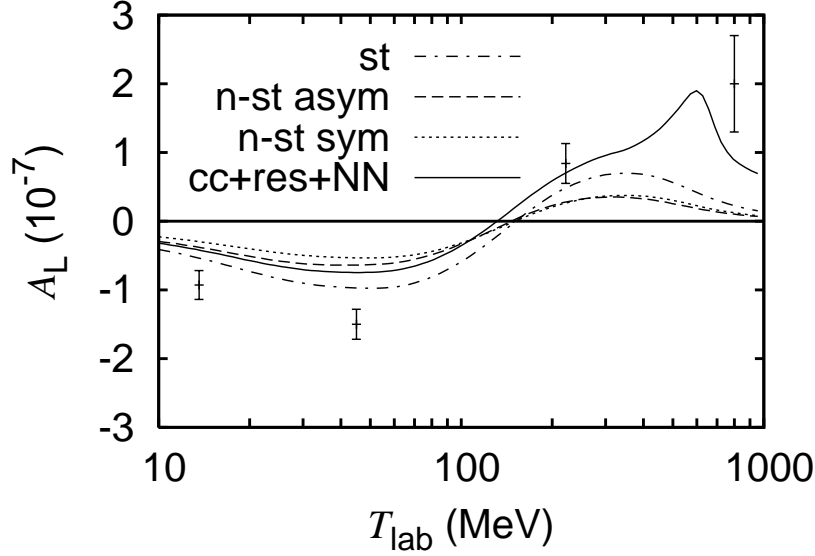


FIG. 7: Model dependence of PNC TPE using the DDH "best" value for the $h_\pi^{(1)}$. The solid line is the sum of coupled channels, the residual part, and the NN crossed contributions. The dash-dotted line is the static, dotted non-static symmetric, and the dashed non-static asymmetric PNC TPE as discussed in the text.

of the previous diagrammatic integrals of Eq. (7) this rearrangement means

$$\tilde{U}_{N\Delta}^{\text{CC}}(\mathbf{q}) = -\frac{32f_\pi^3}{25\sqrt{2}\pi^2m_\pi^3} \int_0^\infty dk k^4 (\mathcal{D}_{N\Delta}^{\text{B}} + \mathcal{D}_{N\Delta}^{\text{C}}), \quad (16)$$

$$\tilde{U}_{N\Delta}^{\text{RES}}(\mathbf{q}) = \frac{128f_\pi^3}{75\sqrt{2}\pi^2m_\pi^3} \int_0^\infty dk k^4 \mathcal{D}_{N\Delta}^{\text{C}}. \quad (17)$$

Here the part (16) is to be treated in the coupled-channels approach; the same term would arise from the iteration of the strong Eq. (18) and weak Eq. (19) OPE transition potentials. One advantage of coupled channels is that different centrifugal barriers related to the orbital angular momenta are automatically taken into account. Therefore, coupled channels results are state dependent. Also opening of different channels causes energy dependence, which cannot be simulated by energy independent potentials alone.

The first two basic Hamiltonians, Eqs. (1) and (2), lead to the strong OPE transition ($NN \leftrightarrow N\Delta$) potential

$$V_{N\Delta\pi}^{\text{PC}}(\mathbf{r}) = \frac{f_\pi^* f_\pi}{m_\pi^2} \left[(\mathbf{S}_1 \cdot \nabla)(\boldsymbol{\sigma}_2 \cdot \nabla) \mathbf{T}_1 \cdot \boldsymbol{\tau}_2 + (\boldsymbol{\sigma}_1 \cdot \nabla)(\mathbf{S}_2 \cdot \nabla) \mathbf{T}_1 \cdot \mathbf{T}_2 \right] Y_\pi(\mathbf{r}), \quad (18)$$

whereas from Eqs. (2) and (3) we get the weak OPE transition ($NN \leftrightarrow N\Delta$) potential

$$V_{\pi N\Delta}^{\text{PNC}}(\mathbf{r}) = \frac{h_\pi^{(1)} f_\pi^*}{\sqrt{2}m_\pi} \left[(\boldsymbol{\tau}_1 \times \mathbf{T}_2)_0 \hat{\mathbf{r}} \cdot \mathbf{S}_2 + (\mathbf{T}_1 \times \boldsymbol{\tau}_2)_0 \hat{\mathbf{r}} \cdot \mathbf{S}_1 \right] \frac{\partial}{\partial r} Y_\pi(\mathbf{r}). \quad (19)$$

Iterating these two should give the effect of the potential (16), a claim borne out in a comparison of the dashed and solid (coupled channels + residual + crossed NN) curves in

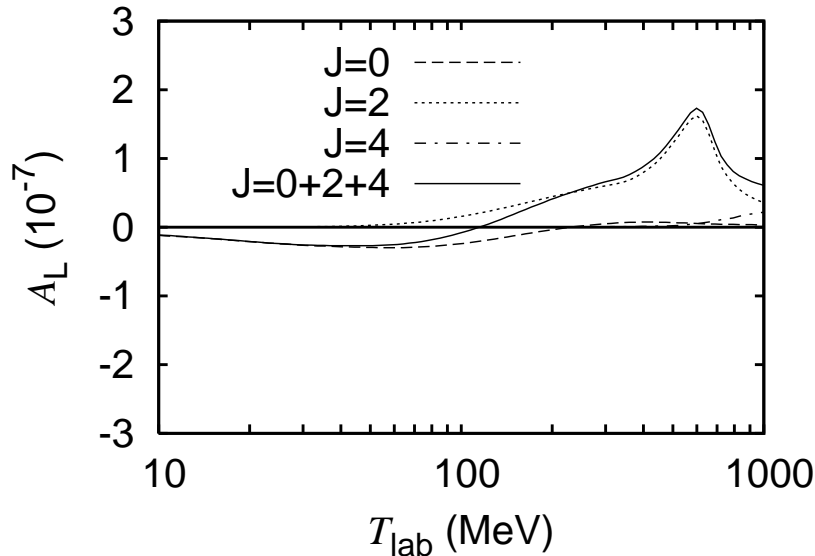


FIG. 8: Partial wave contributions to \bar{A}_L from PNC TPE using the coupled-channels approach and the DDH "best" value for the $h_\pi^{(1)}$.

Fig. 7. At low energies the result is very similar to the non-static asymmetric potential result but deviates drastically in energy dependence in particular in the proximity of the ΔN threshold.

It is of interest to study in more detail the dip at 600 MeV in Fig. 7. This kind of cusp structures arise in dynamical coupled channels calculations (as isospin one "dibaryon" resonances in the case of ΔN thresholds giving rise to maxima e.g. in pion production), but the present one is somewhat sharper than the wide maximum seen in Ref. [11]. However, there it was produced by PNC ρ exchange interfering with the strong transition involving both pion and a destructive ρ . In the present case, to be consistent with the TPE potential, we have exclusively the long ranged pion exchange in both transition potentials without damping other than the form factor. The structure is due to the favoured transition $^1D_2(pp) \leftrightarrow ^5S_2(\Delta^{++}n) \leftrightarrow ^3P_2(pp)$ through the intermediate state without a centrifugal barrier. The other intermediate ΔN states coupling with tensor-coupled states and with centrifugal barrier are not particularly favoured [30]. These phenomenological arguments are confirmed in Fig. 8, which shows splitting the above total result into partial wave amplitudes: the structure is not seen in the otherwise dominant $J = 0$ amplitude, which has the same structure (dictated by strong interaction [9]) as for other potentials.

III. CONCLUSION

We evaluated the PNC TPEP for the elastic pp scattering and calculated the longitudinal asymmetry \bar{A}_L . Compared to the local contributions of the PNC ω and ρ exchanges our results are of the same order indicating that also this mechanism should be seriously considered in interpreting PNC data. With the old DDH couplings [1] this additional contribution leads to an overestimate, but the newer ones [2] can give a tolerable agreement (though we do not include nonlocal PNC here) especially, if non-static effects are included. However the DDH and FCDH "best" values for the $h_\pi^{(1)}$ might be too large in the light of the experimental

restrictions given by the ^{18}F parity violating measurements [31, 32], which bound the upper limit in the range $|h_\pi^{(1)}| \leq 1.5 \times 10^{-7}$. Some theoretical predictions are also within this limit [33, 34, 35]. Further, one should note that the relative sign of the pion strong and weak coupling may be unknown in the vertex definitions (1)–(3) even if the weak magnitude were given. The knowledge of this coupling is essential, since the pions are more than five times lighter than the vector mesons and thus the PNC TPE presumably represents the longest range part of the weak interaction in pp scattering.

In particular relating to the TRIUMF experiment at 221.3 MeV we get at that energy the TPE contribution 0.48 to \bar{A}_L in the static model and in the nonstatic "symmetric" model 0.26 (0.28 in the "asymmetric" one). These may set rather realistic limits though the even larger result 0.70 using the coupled channels model should be noted. However, these are obtained using the older DDH coupling $h_\pi^{(1)} = 4.6 \cdot 10^{-7}$ and can be easily scaled for the value from the FCDH analysis $h_\pi^{(1)} = 2.7 \cdot 10^{-7}$ or any other.

The long ranged OPE transition potential produces also a manifest cusp peak at 600 MeV in a coupled channels calculation. Whether or not this will be diminished in the presence of vector mesons will be discussed in a subsequent work [36]. There are two competing effects: destructive interference from the ρ exchange in the strong transition potential and the contribution from the ρ in the PNC transition as discussed earlier [11]. In any case, as suggested in Ref. [11] an experimental point between the TRIUMF and Los Alamos energies would be of interest.

Acknowledgments

We wish to acknowledge the hospitality of Forschungszentrum Jülich, Germany, where this work was partly done and partial support from the Academy of Finland (grant 121892).

-
- [1] B. Desplanques, J. F. Donoghue, and B. R. Holstein, *Ann. Phys.* **124**, 449 (1980).
 - [2] G. B. Feldman, G. A. Crawford, J. Dubach, and B. R. Holstein, *Phys. Rev. C* **43**, 836 (1991).
 - [3] E. G. Adelberger and W. C. Haxton, *Annu. Rev. Nucl. Part. Sci.* **35**, 501 (1985).
 - [4] B. Desplanques, *Phys. Rep.* **297**, 1 (1998).
 - [5] S. Kistryn et al., *Phys. Rev. Lett.* **58**, 1616 (1987).
 - [6] P. Eversheim et al., *Phys. Rev. Lett. B* **256**, 11 (1991).
 - [7] V. Yuan et al., *Phys. Rev. Lett.* **57**, 1680 (1986).
 - [8] A. R. Berdoz et al., *Phys. Rev. C* **68**, 034004 (2003).
 - [9] M. Simonius, *Can. J. Phys* **66**, 548 (1988).
 - [10] G. Barton, *Nuovo Cimento* **19**, 512 (1961).
 - [11] M. J. Iqbal and J. A. Niskanen, *Phys. Rev. C* **49**, 1 (1994).
 - [12] B. Desplanques, *Phys. Lett. B* **41**, 461 (1972).
 - [13] D. O. Riska and H. J. Pirner, *Phys. Lett. B* **44**, 151 (1973).
 - [14] R. R. Silbar, W. M. Kloet, L. S. Kisslinger, and J. Dubach, *Phys. Rev. C* **40**, 2218 (1989).
 - [15] W. M. Kloet, R. R. Silbar, and J. A. Tjon, *Phys. Rev. C* **41**, 2263 (1990).
 - [16] N. Kaiser, *Phys. Rev. C* **76**, 047001 (2007).
 - [17] E. M. Henley, *Phys. Rev. Lett.* **27**, 542 (1971).
 - [18] G. E. Brown and W. Weise, *Phys. Rep.* **22**, 279 (1975).

- [19] R. Machleidt, K. Holinde, and C. Elster, Phys. Rep. **149**, 1 (1987).
- [20] S. A. Coon and M. D. Scadron, Phys. Rev. C **23**, 1150 (1981).
- [21] J. A. Niskanen, Phys. Lett. B **107**, 344 (1981).
- [22] A. W. Thomas and K. Holinde, Phys. Rev. Lett. **63**, 2025 (1989).
- [23] K. Holinde and A. W. Thomas, Phys. Rev. C **42**, 1195 (1990).
- [24] J. A. Niskanen, Phys. Rev. C **45**, 2648 (1992).
- [25] R. V. Reid, Ann. Phys. (N.Y.) **50**, 411 (1968).
- [26] R. A. Arndt, J. S. HyslopIII, and L. D. Roper, Phys. Rev. D **35**, 128 (1987).
- [27] D. E. Driscoll and G. A. Miller, Phys. Rev. C **39**, 1951 (1989).
- [28] J. Carlson, R. Schiavilla, V. R. Brown, and B. F. Gibson, Phys. Rev. C **65**, 035502 (2002).
- [29] P. D. Eversheim, private communication (1994), quoted by W. D. Ramsay
oai:arXiv.org:nucl-ex/0210008 (2002).
- [30] J. A. Niskanen, Phys. Lett. B **112**, 17 (1982).
- [31] S. A. Page et al., Phys. Rev. C **35**, 1119 (1987).
- [32] M. Bini et al., Phys. Rev. Lett. **55**, 795 (1985).
- [33] N. Kaiser and U. Meissner, Nucl. Phys. A **499**, 699 (1989).
- [34] V. M. Dubovik and S. V. Zenkin, Ann. Phys. (N.Y.) **172**, 100 (1986).
- [35] M. J. Iqbal and J. A. Niskanen, Phys. Rev. C **42**, 1872 (1990).
- [36] M. J. Iqbal, J. A. Niskanen, and T. M. Partanen, Work in progress (2008).